Case Studies of a MODIS-Based Potential Evapotranspiration Input to the Sacramento Soil Moisture Accounting Model

ANGELA L. BOWMAN AND KRISTIE J. FRANZ

Department of Geological and Atmospheric Sciences, Iowa State University, Ames, Iowa

TERRI S. HOGUE

Department of Civil and Environmental Engineering, Colorado School of Mines, Golden, Colorado

(Manuscript received 30 August 2016, in final form 16 November 2016)

ABSTRACT

A satellite-based potential evapotranspiration (PET) estimate derived from Moderate Resolution Imaging Spectroradiometer (MODIS) observations was tested for input to the spatially lumped and gridded Sacramento Soil Moisture Accounting (SAC-SMA) model. The 15 forecast points within the National Weather Service (NWS) North Central River Forecast Center (NCRFC) forecasting region were the basis for this analysis. Through a series of case studies, the MODIS-derived PET estimate (M-PET) was evaluated for input to the SAC-SMA model by comparing streamflow simulations with those from traditional SAC-SMA evapotranspiration (ET) demand. Two prior studies have evaluated the M-PET data 1) to compute new long-term average ET demand values and 2) to input a time series (i.e., daily time-varying PET) to the NWS Hydrology Laboratory–Research Distributed Hydrologic Model (HL-RDHM), a spatially distributed version of the SAC-SMA model. This current paper presents results from a third test in which the M-PET time series is input to the lumped SAC-SMA model. In all cases, evaluation is between the M-PET data and the long-term average values used by the NWS. Similar to prior studies, results of the current analysis are mixed with improved model evaluation statistics for 4 of 15 basins tested. Of the three cases, using the time-varying M-PET as input to the distributed SAC-SMA model led to the most promising results, with model simulations that are at least as good as those when using the SAC-SMA ET demand. Analyses of the model-simulated ET suggest that the time-varying M-PET input may produce a more physically realistic representation of ET processes in both the lumped and distributed versions of the SAC-SMA model.

1. Introduction

Historically, spatially, and temporally relevant meteorological data needed to compute daily potential evapotranspiration (PET) at the watershed scale has been lacking (Burnash 1995; Fowler 2002). As a result, PET inputs into hydrologic models typically consist of long-term averages rather than time-varying values. This practice is generally acceptable, as time-varying PET inputs appear to add little value to streamflow simulations (Burnash 1995; Oudin et al. 2005a). Oudin et al. (2005a,b) evaluated the sensitivity of PET inputs into four rainfall–runoff models and concluded that long-term average PET inputs result in adequate streamflow simulations, thus negating the need for time-varying PET inputs. At the same time, though, for the purposes of operational use, they questioned whether hydrologic models would be more effective with time-varying inputs that have better temporal resolution. In a 1981 study (Lindsey and Farnsworth 1997), the National Weather Service (NWS) compared the use of daily varying versus mean monthly PET inputs to hydrologic forecast models and found overall improved streamflow simulations using the daily PET estimates. Recent advances in estimating daily PET from satellite (Kim and Hogue 2008, 2012) and modeling systems (Xia et al. 2015a,b) have made access to spatially relevant PET for operational modeling possible. Thus, there is a need to revisit the potential benefits and limitations of applying a time-varying PET in operational streamflow prediction.

Previous and current work explores the application of a daily, 500-m, Moderate Resolution Imaging Spectroradiometer (MODIS)-derived PET estimate developed

Corresponding author e-mail: Angela L. Bowman, albowman@iastate.edu

DOI: 10.1175/JHM-D-16-0214.1

by Kim and Hogue (2008, 2012) for application in NWS streamflow forecast models in watersheds of the upper Mississippi and Red River basins (Bowman et al. 2015; Spies et al. 2015; Barik et al. 2016). The NWS applies the current operational streamflow prediction model—the Sacramento Soil Moisture Accounting (SAC-SMA) model—in a spatially lumped manner and inputs monthly or daily average values of evapotranspiration (ET) demand derived from historical values (Burnash 1995; Anderson 2002). A spatially distributed version of the SAC-SMA model, called the Hydrology Laboratory–Research Distributed Hydrologic Model (HL-RDHM), also uses gridded long-term ET demand values created from maps of potential evaporation in Farnsworth et al. (1982). The MODIS-derived PET estimates (M-PET) have been explored as input to each version of the SAC-SMA model in prior work (cases 1 and 2, described below). The current work adds a third analysis to finalize all possible current applications of the M-PET for operational modeling. The three cases are as follows:

- Case 1: Bowman et al. (2015) tested the application of the M-PET data for use in replacing the long-term average SAC-SMA ET demand values (monthly scale) used by the North Central River Forecast Center (NCRFC) for 15 basins. New values of SAC-SMA ET demand were computed from the M-PET and then input to the spatially lumped SAC-SMA model. The purpose of this test was to explore use of the M-PET within the framework of current operational practice.
- Case 2: Spies et al. (2015) tested the M-PET time series (i.e., daily time-varying PET) as input to the distributed SAC-SMA model in the HL-RDHM after regridding the data to the 4-km model domain. This work explores the potential application of M-PET for future forecast applications, which may include use of a distributed hydrologic model.
- Case 3: The current analysis tested the application of the M-PET time series (i.e., daily time-varying PET) as input to the spatially lumped SAC-SMA model as a possible replacement for the long-term monthly average SAC-SMA ET demand values used under current operations. This study represents an intermediary step between cases 1 and 2.

Here we present results from case 3 along with a comparison of the outcomes from all three studies.

2. Methods

a. Study basins and PET data

The study basins tested here are the same 15 forecast points used in case 1 (Fig. 1) while 13 basins were tested in case 2. Mean daily values of precipitation, runoff, and the two PET inputs for each basin for the evaluation period from 1 May to 30 September are presented (Table 1). All forecast points fall within the NCRFC region in the upper Mississippi and Red River basins.

Our baseline for evaluation in case 3 was the application of SAC-SMA ET demand values for each forecast point provided by the NCRFC (NC-PET). For case 2, the baseline for evaluation was the a priori parameter grids developed by the Office of Hydrologic Development (OHD). The definition of the SAC-SMA ET demand is evaporation that occurs

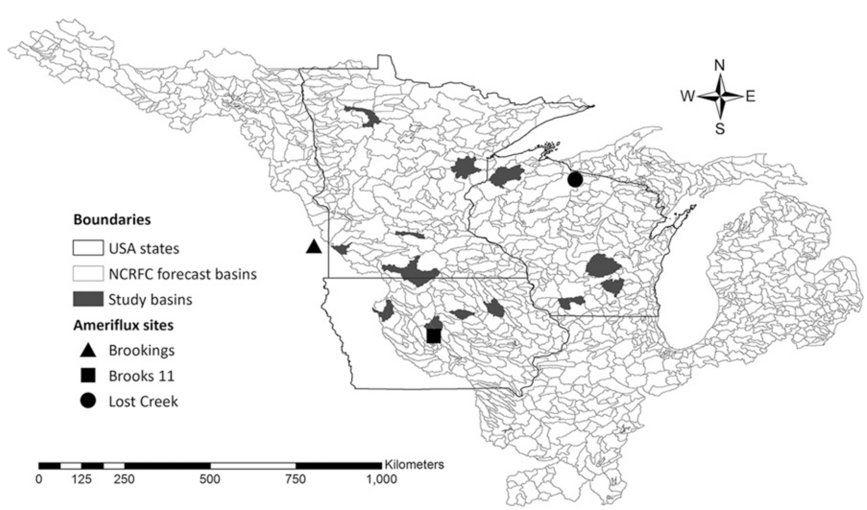

FIG. 1. NCRFC forecast basins (outline), study basins (gray), and AmeriFlux sites used in the current study.

TABLE 1. Study basins with associated NCRFC forecast point ID and USGS gauging station number. Basin size and characteristics including mean daily precipitation, basin runoff, and PET (mm) are presented for the period from 1 May to 30 Sep for WY 2003–08.

Basin	NCRFC forecast point ID	USGS gauging station No.	Basin size (km^2)	Mean daily precipitation (mm)	Mean daily runoff (mm)	Mean daily NC-PET (mm)	Mean daily M-PET (mm)
Beaver Creek	NHRI4	05463000	899	3.77	1.29	4.50	6.09
North Raccoon River	SCRI4	05482300	1813	3.35	0.87	3.80	6.23
South Skunk River	AMEI4	05470000	816	3.84	1.04	4.00	6.21
Squaw Creek	AMWI4	05470500	530	4.00	1.11	3.98	6.19
Wapsipinicon River	IDPI4	05421000	2714	3.75	1.13	4.16	5.99
Blue Earth River	RAPM5	05320000	6242	3.45	0.66	3.44	6.12
Clearwater River	PLUM5	05078000	2847	2.61	0.15	4.24	5.53
High Island Creek	HICM5	05327000	617	3.03	0.45	3.62	6.04
Kettle River	SANM5	05336700	2248	2.96	0.65	3.44	5.78
Redwood River	MMLM5	05315000	671	2.90	0.27	3.78	6.06
Crawfish River	MILW3	05426000	1974	3.47	0.87	4.26	5.79
East Branch Pecatonica River	BCHW3	05433000	572	3.42	0.86	4.52	5.91
Fox River	BERW3	04073500	3471	3.09	0.91	3.98	5.99
Pecatonica River	DARW3	05432500	707	3.64	0.95	4.44	5.89
St. Croix River	DANW3	05333500	4092	2.77	0.64	3.86	5.83

when moisture supply is not limited given existing vegetation type and activity level (Anderson 2002). The NC-PET values are the product of potential evaporation (PE), typically from climatological means (i.e., raw pan evaporation data), and monthly PE vegetation adjustment factors. The NC-PET input to the SAC-SMA model remains static from year to year.

The daily, 500-m-resolution, MODIS-derived PET estimates were spatially averaged to get basin average M-PET for each of the 15 sites. Net radiation, air temperature, and soil heat flux were estimated using nine MODIS products and input to the Priestley–Taylor formula (Kim and Hogue 2008, 2012; Bowman et al. 2015; Spies et al. 2015; Barik et al. 2016). The daily M-PET was derived from 1 May to 30 September. For the few days with missing M-PET values, values were interpolated from available data. The study period [water years (WY) 2003–08] coincided with the availability of the satellite-derived M-PET data as well as quality-controlled historical model inputs of precipitation and temperature provided by the NCRFC for the spatially lumped SAC-SMA model.

b. SAC-SMA model

The SAC-SMA model is a conceptual rainfall–runoff model that represents the hydrologically active soil zone as two layers, a thin upper zone and a thicker lower zone (Burnash et al. 1973; Burnash 1995; Koren et al. 1999; Anderson 2002). Each layer is composed of tension water representing water driven by ET and diffusion and free water representing water driven by gravitational forces. The model-simulated ET is a function of the SAC-SMA ET demand and the available tension water, computed from the tension water storages in the upper and lower zones. Depletion in the upper-zone tension water occurs only through evaporation; once the upper-zone tension reaches saturation, water then flows to the upper-zone free water. From the upper-zone free water both percolation to the lower zone and interflow occurs. Surface runoff begins once the upper-zone free water reaches saturation.

c. Evaluation of the PET inputs (NC-PET and M-PET)

The PET inputs (NC-PET and M-PET) from three study basins were evaluated at the point-scale against ''observed'' average daily PET calculated using the Priestley–Taylor formula and observations from the nearest AmeriFlux sites: Brooks 11 (Squaw Creek basin), Brookings (Redwood River basin), and Lost Creek (St. Croix River basin) (Fig. 1). In addition, comparisons were made of the model–simulated ET from both PET inputs to latent heat flux observations from the same three AmeriFlux sites. Finally, model-simulated discharge was compared to USGS mean daily observed values for each forecasting point. Percent bias (%Bias), mean absolute error (MAE), and Nash–Sutcliffe efficiency (NSE; Nash and Sutcliffe 1970) statistics were computed for the period from 1 May to 30 September.

The SAC-SMA model generally requires site- and data-specific calibration as this model is sensitive to the input data used in the calibration process (Anderson 2002). Therefore, the SAC-SMA model calibration was completed for each basin and each PET input using a calibration period from 1 October 2005 to 30 September 2008. The verification period was from 1 October 2002 to 30 September 2005 with a 1-yr spinup period.

d. Calibration methods utilized for each case study

In each case study, calibration of the model was computed to each PET input and for each forecasting point. For the spatially lumped SAC-SMA model applications (cases 1 and 3), the calibration procedure followed the Multi-Step Automatic Calibration Scheme (MACS) for 13 SAC-SMA model and five SNOW-17 model parameters (Hogue et al. 2000, 2006). The MACS procedure is a three-step process in which all parameters are first calibrated using the log square error objective function to obtain overall fit to the observed hydrograph. Next, those parameters that most affect high flows are calibrated using the root-mean-square error objective function. A final step is completed to calibrate the parameters affecting the low flows using the log square error.

For the distributed SAC-SMA model application (case 2), the calibration procedure followed the automated stepwise line search (SLS; Kuzmin et al. 2008; NWS 2009). Parameter multipliers, rather than the parameter values, were calibrated and applied to the a priori parameter grids with the same multiplier applied to each grid cell. A multiscale objective function was utilized and is discussed in further detail in Spies et al. (2015).

To the extent possible, testing of the M-PET was similar in all cases. PET inputs and model-simulated ET from each case was evaluated against PET estimates and latent heat flux observations from ground-based data at AmeriFlux sites (Fig. 1). The NC-PET (SAC-SMA ET demand) data were the baseline for evaluating the M-PET data and their application in the SAC-SMA model. The M-PET data were applied for the period from 1 May to 30 September of each year, spanning the months when plant productivity is at its highest and ET is most significant to the regional water balance in the study region. SAC-SMA ET demand values were used for the period between 1 October and 30 April. It is worth noting that NC-PET values averaged less than 1 mm day^{-1} during the October–April period, and extensive cloud cover prevented derivation of M-PET values for many days in the winter. In all three cases, the daily NC-PET and M-PET values were divided evenly over each 6-h simulation time step of the SAC-SMA model. All data comparisons and model analysis occurred for the months between 1 May and 30 September.

TABLE 2. Case 3 R^2 and bias (mm) statistics for the period from 1 May to 30 Sep for WY 2003–08. PET estimated from the Priestley–Taylor formula and ground-based observations are compared with the NC-PET and M-PET model inputs. Model-simulated ET values from the NC-PET and M-PET inputs are compared with ground-based latent heat flux for Squaw Creek, Redwood River, and St. Croix River.

	PET		Simulated ET	
Case 3	NC-PET	M-PET	NC-PET	M-PET
Squaw Creek				
R^2	0.03	0.25	0.28	0.10
Bias (mm)	−1.14	1.15	0.60	0.64
Redwood River				
R^2	0.24	0.23	0.16	0.11
Bias (mm)	−1.41	0.87	−0.79	−0.77
St. Croix River				
R^2	0.02	0.15	0.19	0.03
Bias (mm)	−3.96	−1.08	1.46	1.80

3. Results and discussion

a. Case 3: M-PET PET and model-simulated ET

Evaluating the PET inputs (M-PET and NC-PET), the average coefficient of determination R^2 from the three sites with associated AmeriFlux data is higher for the M-PET ($R^2 = 0.21$) than the NC-PET ($R^2 = 0.10$) when compared with the ‘‘observed’’ PET (Fig. 1, Table 2). Kim and Hogue (2008) found an average point-to-pixel correlation for PET of $R^2 = 0.87$ at four flux tower sites across the United States. Note that their study included the winter months. In our study, however, only the period from 1 May to 30 September was included, which may explain the lower correlations. In our evaluation of the PET inputs, the results from case 3 were similar to the findings from cases 1 and 2 that showed the R^2 from the M-PET were better overall than the NC-PET. Bowman et al. (2015) report an M-PET $R^2 = 0.50$ and NC-PET $R^2 = 0.33$ (case 1), while Spies et al. (2015) report an M-PET $R^2 = 0.66$ and NC-PET $R^2 = 0.13$ (case 2).

The PET comparison at Brooks 11 (Squaw Creek) and Brookings (Redwood River) showed negative bias for the NC-PET and positive bias for the M-PET, while at Lost Creek (St. Croix River) bias was negative for both inputs (Table 2). The magnitude of bias was smaller on average for the M-PET (1.03 mm) compared to NC-PET (2.17 mm). The tendency for the M-PET method to produce PET estimates with positive bias compared to ground-based estimates was a common observation among other studies (Kim and Hogue 2008, 2012; Barik et al. 2016; Xia et al. 2016). Likewise, across the case studies the PET data used by the NWS were consistently lower than the ‘‘observed’’ PET, in some instances by as much as 4 mm day^{-1} (Table 2; Bowman et al. 2015; Spies et al. 2015). Several authors report an inability to close the

TABLE 3. Case 3 model evaluation statistics for streamflow simulations that show %Bias, MAE ($m^3 s^{-1}$), and NSE for the calibration period (WY 2006–08) and the verification period (WY 2003–05).

	Calibration						Verification					
	%Bias (%)		MAE		NSE		%Bias (%)		MAE		NSE	
Basin	NC-PET	M-PET	NC-PET	M-PET	NC-PET	M-PET	NC-PET	M-PET	NC-PET	M-PET	NC-PET	M-PET
Beaver Creek	−26.25	−11.06	5.80	5.70	0.74	0.74	−28.45	−1.04	4.15	4.28	0.58	0.72
North Raccoon River	−23.97	−18.91	7.30	8.90	0.72	0.65	−28.03	−40.80	8.77	11.62	0.65	0.40
South Skunk River	2.98	−18.49	4.26	4.32	0.84	0.82	9.96	−18.31	2.27	2.34	0.84	0.77
Squaw Creek	−10.26	−3.91	4.42	3.09	0.76	0.86	−25.54	−4.36	2.79	2.40	0.58	0.69
Wapsipinicon River	−26.21	−27.44	20.27	20.96	0.53	0.49	−30.73	−31.57	16.94	17.45	0.45	0.41
Blue Earth River	−10.60	−21.98	18.31	22.77	0.70	0.40	−5.53	−33.62	15.90	25.03	0.82	0.63
Clearwater River	−7.22	−28.53	2.09	2.62	0.69	0.54	−40.50	−48.64	2.96	3.27	0.30	0.24
High Island Creek	−8.62	−14.88	0.83	1.27	0.76	0.58	−47.96	−57.96	2.88	3.18	0.36	0.27
Kettle River	−7.41	−39.21	7.18	6.03	0.56	0.51	−24.77	−77.98	10.67	16.57	0.45	<0
Redwood River	−31.49	−33.80	1.05	1.26	0.51	0.27	−3.68	−9.96	0.94	1.04	0.55	0.38
Crawfish River	−5.22	−10.24	8.93	8.39	0.80	0.78	−5.81	−13.05	4.58	5.68	0.91	0.83
East Branch Pecatonica River	−19.34	−12.77	1.58	1.43	0.80	0.80	−9.41	−8.67	0.62	1.14	0.69	0.70
Fox River	2.59	−19.60	7.41	9.76	0.89	0.76	−13.66	−36.09	7.58	13.76	0.86	0.62
Pecatonica River	−16.25	−17.94	2.08	2.77	0.86	0.81	−12.91	−18.50	1.33	1.55	0.75	0.78
St. Croix River	12.78	−28.73	5.31	7.16	0.78	0.62	−8.58	−38.79	6.48	13.97	0.73	0.23

energy balance at AmeriFlux sites, and it may be one factor contributing to bias in the PET estimates (Stoy et al. 2013; Tang et al. 2011; Xia et al. 2015b). Xia et al. (2015b), in particular, used corrections for monthly mean ET observations to close the energy balance and assess bias in their data.

For case 3, comparisons between the model-simulated ET for both PET inputs and the ground-based latent heat flux observations from the three AmeriFlux sites are reported (Fig. 1). The M-PET model-simulated ET had poorer correlation ($R^2 = 0.08$) than the NC-PET ($R^2 = 0.21$, Table 2), and on average, bias is slightly larger for the M-PET (1.07 mm) compared to NC-PET (0.95 mm). The case 3 correlation for model-simulated ET was similar to both case 1 (M-PET $R^2 = 0.08$, NC-PET $R^2 = 0.23$) and case 2 (M-PET $R^2 = 0.18$, NC-PET $R^2 = 0.18$), in which the simulated ET from the M-PET performed slightly poorer overall. Because of the high bias of the M-PET values in each case relative to the ground-based data, the degree of scatter in simulated ET was higher with the M-PET for all sites and was the likely cause of the lower R^2 values. However, Xia et al. (2015a) report that flux towers in the continental United States tend to underestimate ET (latent heat flux) by as much as 30%. Accounting for this potential error, the model-simulated ET from the M-PET could be more reflective of ET occurring in these watersheds than these comparisons may show.

b. *Case 3: Simulated discharge*

Simulated discharge produced from the M-PET input for the calibration period had larger %Bias, ranging from −39.2% to −3.9%, compared to the simulation using NC-PET input, which ranged from −26.3% to +3.0% (Table 3). Lower %Bias compared to NC-PET occurred with the M-PET for only four basins (Beaver Creek, North Raccoon River, Squaw Creek, and East Branch Pecatonica River). There was a small improvement in mean error (average less than 1 mm day^{-1}) for five basins (Beaver Creek, Squaw Creek, Kettle River, Crawfish River, and East Branch Pecatonica River) when using the M-PET input.

Discharge was largely undersimulated by both the NC-PET and M-PET inputs for the verification period; examples include Beaver Creek and Kettle River (Fig. 2). The South Skunk River NC-PET simulation is the exception, in which discharge is overestimated (Table 3). Across all basins and all PET inputs, simulations tended to underestimate high flows, while low flows in general were slightly overestimated. Beaver Creek (Fig. 2a) had the greatest improvement in streamflow with the M-PET, and the Kettle River (Fig. 2b) had the least improvement in streamflow with the M-PET. The M-PET produced smaller biases in simulated discharge than the NC-PET in three basins (Beaver Creek, Squaw Creek, and East Branch Pecatonica River) and lower mean error by less than 0.50 mm for one basin (Squaw Creek). For the remaining basins, NC-PET daily mean error was on average 2.50 mm lower than the M-PET. NSE scores were higher overall with the NC-PET (0.63) than the M-PET (0.55), though most showed similar model performance with either PET input.

c. *Comparison of discharge simulations: Case 1, case 2, and case 3*

Case 2 had the lowest average %Bias (26%) of the three cases with the M-PET inputs and was the only

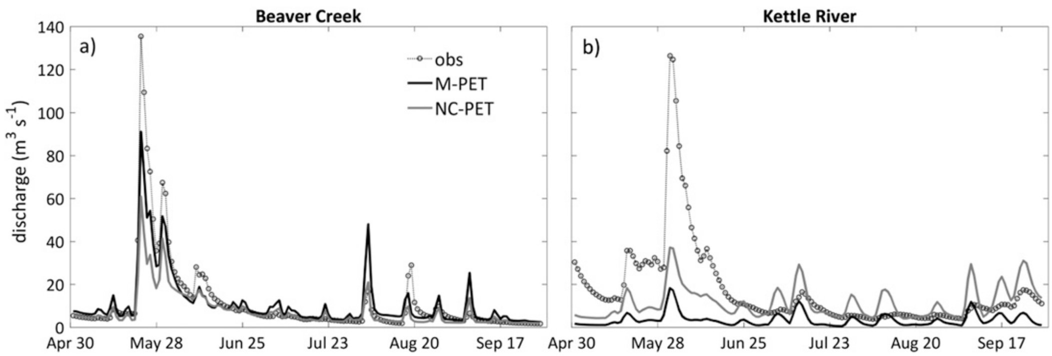

FIG. 2. Discharge plots from case 3 showing the M-PET (black line) and NC-PET (gray line) simulations compared with the observed (dotted line with circles) from 1 May to 30 Sep 2004 for (a) Beaver Creek, the best performing basin in terms of %Bias, and (b) Kettle River, the worst performing basin in terms of %Bias.

scenario in which the average M-PET bias produced model simulations that overestimated streamflow (i.e., had positive bias). Positive bias occurred for three basins (Beaver Creek, Redwood River, and East Branch Pecatonica River), and each showed improvement in the simulated discharge over the NC-PET. The case 1 application of the M-PET produced the worst streamflow biases with observed discharge underestimated on average by 40% and as much as 60% in one basin (High Island Creek).

NSE scores were improved or nearly identical when using the M-PET data as compared to the NC-PET data in seven basins for case 2 and four basins for case 3 (Fig. 3). No basin showed improvement in NSE scores for case 1. Based on comparison between the three cases, the M-PET time series shows the most promise for applications to the distributed SAC-SMA model. In addition, direct input of the daily M-PET time series to the lumped model was more successful than using the data to update the long-term monthly average values. The greatest overall improvement in NSE occurred for the Blue Earth River in case 2 while the East Branch Pecatonica River and the Pecatonica River have improved NSE scores for both case 2 and case 3.

4. Conclusions

With the case study presented here, we completed a series of tests in which we examined the application of a satellite-based PET estimate (M-PET) with the following results:

- Case 1: Testing new ET demand curves as input to the lumped SAC-SMA model resulted in consistent underestimation of simulated discharge and did not lead to improved performance as compared to the current operational PET data.
- Case 2: Testing the time-varying M-PET as input to the distributed SAC-SMA model produced results that are able to match model performance when using inputs of long-term average ET demand (NC-PET). In

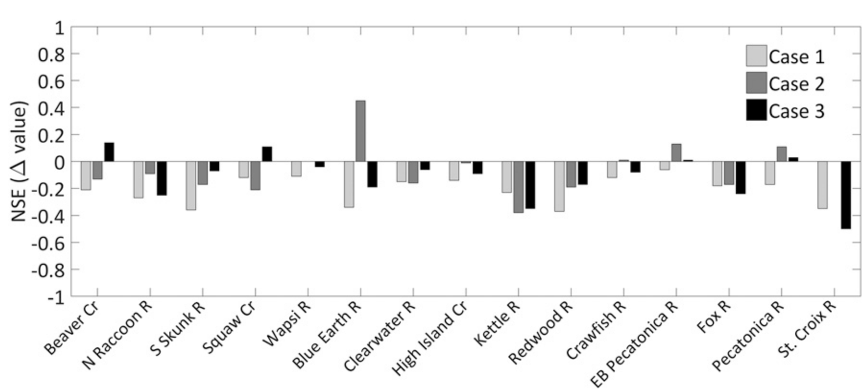

FIG. 3. NSE delta comparison showing the difference between NC-PET and M-PET discharge simulations for case 1 (Bowman et al. 2015), case 2 (Spies et al.2015), and case 3 (current study). Positive values indicate that the M-PET had a higher NSE value than the NC-PET. Negative values indicate that the NC-PET had a higher NSE value than the M-PET.

some cases, performance improved with M-PET even though simulated discharge was still underestimated.

- Case 3: Testing the time-varying M-PET as input to the lumped SAC-SMA model produced results that underestimated simulated discharge, often with overall larger bias when compared to the SAC-SMA ET demand inputs. This application of the M-PET data was more successful than case 1 and led to improved results in four basins, though was less successful than case 2 in terms of overall model efficiency.

Each test failed to show consistent improvement in discharge simulations across all basins. However, the application of time-varying M-PET input in the distributed modeling framework of the SAC-SMA model (case 2; Spies et al. 2015) had the best overall results and shows potential for future application of the M-PET. Case 3 also shows promise, as application of the time-varying PET input to the lumped SAC-SMA model performed well for some basins. Case 1 is not a recommended application of M-PET based on simulated discharge results. Analyses of the simulated ET indicated that the time-varying M-PET input (cases 2 and 3) produced a more physically realistic representation of ET processes in the model, suggesting that use of the M-PET may improve one aspect of the model simulation (ET) at the expense of another (discharge). Results from the presented case studies further our understanding of the potential for and current limitations of using satellite-based inputs in operational streamflow prediction.

Acknowledgments. Financial support for this work was provided by a NASA New Investigator Program Grant (NNX10AQ77G) and a NASA Research Opportunities in Space and Earth Science (ROSES) Grant (NNX15AB28G). Special thanks to Mike DeWeese and staff at the NCRFC with model assistance and data acquisition and to the anonymous reviewers who greatly improved the manuscript. We also thank the AmeriFlux Research Network PIs who provided observation data used in this work.

REFERENCES

Anderson, E. A., 2002: Calibration of conceptual hydrologic models for use in river forecasting. NWS Doc., 372 pp. [Available online at http://www.nws.noaa.gov/oh/hrl/modelcalibration/1.%20Calibration%20Process/1_Anderson_CalbManual.pdf.]

Barik, M. G., T. S. Hogue, K. J. Franz, and A. M. Kinoshita, 2016: Assessing satellite and ground-based potential evapotranspiration for hydrologic applications in the Colorado River basin. *J. Amer. Water Resour. Assoc.*, **52**, 48–66, doi:10.1111/1752-1688.12370.

Bowman, A. L., K. J. Franz, T. S. Hogue, and A. M. Kinoshita, 2015: MODIS-based potential evapotranspiration demand curves for the Sacramento Soil Moisture Accounting model. *J. Hydrol. Eng.*, **21**, 04015055, doi:10.1061/(ASCE)HE.1943-5584.0001261.

Burnash, R. J. C., 1995: The National Weather Service River Forecast System—Catchment modeling. *Computer Models of Watershed Hydrology*, V. P. Singh, Ed., Water Resources Publications, 311–366.

——, R. L. Ferral, and R. A. McGuire, 1973: A generalized streamflow simulation system: Conceptual models for digital computers. Joint Federal and State River Forecast Center, U.S. National Weather Service, and California Department of Water Resources Tech. Rep., 204 pp.

Farnsworth, R. K., E. S. Thompson, and E. L. Peck, 1982: Evaporation atlas for the contiguous 48 United States. NOAA Tech. Rep. NWS 33, 41 pp. [Available online at www.nws.noaa.gov/oh/hdsc/Technical_reports/TR33.pdf.]

Fowler, A. M., 2002: Assessment of the validity of using mean potential evaporation in computations of long-term soil water balance. *J. Hydrol.*, **256**, 248–263, doi:10.1016/S0022-1694(01)00542-X.

Hogue, T. S., S. Sorooshian, and H. Gupta, 2000: A multistep automatic calibration scheme for river forecasting models. *J. Hydrometeor.*, **1**, 524–542, doi:10.1175/1525-7541(2000)001<0524:AMACSF>2.0.CO;2.

——, L. A. Bastidas, H. V. Gupta, and S. Sorooshian, 2006: Evaluating model performance and parameter behavior for varying levels of land surface model complexity. *Water Resour. Res.*, **42**, W08430, doi:10.1029/2005WR004440.

Kim, J., and T. S. Hogue, 2008: Evaluation of a MODIS-based potential evapotranspiration product at the point scale. *J. Hydrometeor.*, **9**, 444–460, doi:10.1175/2007JHM902.1.

——, and ——, 2012: Improving spatial soil moisture representation through integration of AMSR-E and MODIS products. *IEEE Trans. Geosci. Remote Sens.*, **50**, 446–460, doi:10.1109/TGRS.2011.2161318.

Koren, V. I., B. D. Finnerty, J. C. Schaake, M. B. Smith, D. J. Seo, and Q. Y. Duan, 1999: Scale dependencies of hydrologic models to spatial variability of precipitation. *J. Hydrol.*, **217**, 285–302, doi:10.1016/S0022-1694(98)00231-5.

Kuzmin, V., D. J. Seo, and V. Koren, 2008: Fast and efficient optimization of hydrologic model parameters using a priori estimates and stepwise line search. *J. Hydrol.*, **353**, 109–128, doi:10.1016/j.jhydrol.2008.02.001.

Lindsey, S. D., and R. K. Farnsworth, 1997: Sources of solar radiation estimates and their effect on daily potential evaporation for use in streamflow modeling. *J. Hydrol.*, **201**, 348–366, doi:10.1016/S0022-1694(97)00046-2.

Nash, J. E., and J. V. Sutcliffe, 1970: River flow forecasting through conceptual models part I—A discussion of principles. *J. Hydrol.*, **10**, 282–290, doi:10.1016/0022-1694(70)90255-6.

NWS, 2009: Hydrology Laboratory Research Distributed Hydrologic Model (HL-RDHM) user manual v.2.4.3. NWS Doc., 109 pp. [Available online at http://amazon.nws.noaa.gov/articles/HRL_Pubs_PDF_May12_2009/zc/RDHM_User_Manual.pdf.]

Oudin, L., C. Michel, and F. Anctil, 2005a: Which potential evapotranspiration input for a lumped rainfall–runoff model?: Part 1—Can rainfall–runoff models effectively handle detailed potential evapotranspiration inputs? *J. Hydrol.*, **303**, 275–289, doi:10.1016/j.jhydrol.2004.08.025.

——, F. Hervieu, C. Michel, C. Perrin, V. Andréassian, F. Anctil, and C. Loumagne, 2005b: Which potential evapotranspiration input for a lumped rainfall–runoff model?: Part 2—Towards a simple and efficient potential evapotranspiration model for rainfall–runoff modelling. *J. Hydrol.*, **303**, 290–306, doi:10.1016/j.jhydrol.2004.08.026.

Spies, R. R., K. J. Franz, T. S. Hogue, and A. L. Bowman, 2015: Distributed hydrologic modeling using satellite-derived potential evapotranspiration. *J. Hydrometeor.*, **16**, 129–146, doi:10.1175/JHM-D-14-0047.1.

Stoy, P. C., and Coauthors, 2013: A data-driven analysis of energy balance closure across FLUXNET research sites: The role of landscape scale heterogeneity. *Agric. For. Meteor.*, **171–172**, 137–152, doi:10.1016/j.agrformet.2012.11.004.

Tang, R., Z.-L. Li, and K.-S. Chen, 2011: Validating MODIS-derived land surface evapotranspiration with in situ measurements at two AmeriFlux sites in a semiarid region. *J. Geophys. Res.*, **116**, D04106, doi:10.1029/2010JD014543.

Xia, Y., M. T. Hobbins, Q. Mu, and M. B. Ek, 2015a: Evaluation of NLDAS-2 evapotranspiration against tower flux site observations. *Hydrol. Processes*, **29**, 1757–1771, doi:10.1002/hyp.10299.

——, C. D. Peter-Lidard, M. Huang, H. Wei, and M. Ek, 2015b: Improved NLDAS-2 Noah-simulated hydrometeorological products with an interim run. *Hydrol. Processes*, **29**, 780–792, doi:10.1002/hyp.10190.

——, B. A. Cosgrove, K. E. Mitchell, C. D. Peters-Lidard, M. B. Ek, S. Kumar, D. Mocko, and H. Wei, 2016: Basin-scale assessment of the land surface energy budget in the National Centers for Environmental Prediction operational and research NLDAS-2 systems. *J. Geophys. Res. Atmos.*, **121**, 196–220, doi:10.1002/2015JD023889.